Computationally efficient determination of long term extreme out-of-plane loads for offshore turbines

Natarajan, Anand

Published in:
Scientific Proceedings

Publication date:
2011

Document Version
Publisher's PDF, also known as Version of record

Computationally Efficient Determination of Long Term Extreme Out-of-Plane Loads for Offshore Turbines

Anand Natarajan, Senior Scientist,
Wind Energy Division, Risø DTU, Roskilde, Denmark
anat@risoe.dtu.dk

Abstract

Computationally fast methods to determine the 50 year operating extreme mud line out of plane loads on an offshore turbine are presented. The critical factors that result in the highest extreme out of plane loading at the tower base are presented based on the analysis of results from aeroelastic simulations. These factors are replicated in a simplified frequency domain code that combines the effect of rotor aerodynamics with methods in random vibrations for the peak response of a structure. The wave loading based on the JONSWAP power spectral density (PSD) is applied using both Linear Airy theory and Wheeler stretching. The environmental contour method is used to predict the extreme wave heights for the 50 year operating load. The 50 year mud line out of plane moment using the simplified model is compared with the extreme extrapolated moment obtained using sampled loads from a HAWC2 aero elastic simulation with variations in the number of turbulent wind and irregular wave seeds. The 50 year extreme operating mud line out of plane moment from the simplified code is verified to be within 10% of the corresponding extrapolated extreme load. The impact of soil stiffness can also be readily incorporated into the simplified method. The results provide a verified basis to estimate the extrapolated 50 year extreme mud line loads by using computationally fast models, which account for the major dependencies of the extreme out of plane load.

1. Introduction

The IEC 61400-1 and IEC 61400-3 standards [1,2] for offshore turbines define operating load cases that drive extreme loads. The 50 year extreme operating load identification is characterized by the need to obtain reliable tail data distribution. Reports in literature [3] describe wide variability in the mud line extrapolated bending moment which is dependent on the wind conditions. Also various methods for determining extrapolated extreme loads have been suggested [4]. Invariably the determination of a long term extreme load requires large number of loads simulations. The peak characteristic loads from the simulations at each mean wind speed is identified, to which a Cumulative Distribution Function (CDF) is fit and this is extrapolated to a 50 year probability of exceedance. The extreme load at the mud line is affected by the wave kinematics, rotor nacelle loads, and tower dynamics. Further, the soil interface affects the mud line extreme loads, based on the net reduced support structure stiffness and net damping. A complete study of all these factors would require many repetitions of normal turbulence winds at each mean wind speed by varying the turbulence seed of the wind, the wave significant height and other conditions. However, for the preliminary design of a new offshore turbine, it is beneficial to understand the magnitude of the driving extreme loads on the turbine quickly without having to simulate hundreds of load cases that can take several hours. Thus the requirement for reduced simulations without compromising on the accuracy of the extrapolated load is essential.

The present study used the Upwind 5MW turbine with a rotor diameter of 126m as the reference turbine with a monopile foundation [5]. Different approaches may be encapsulated in a fast solver for extreme loads. A frequency based method is often used as this does not warrant time marching solutions. Reference [6] suggests that the soil stiffness may produce an uncertainty of 10% on

the frequency and therefore the estimation of extreme loads using a frequency based approach can readily highlight the corresponding effects on the extreme load. Some reports in literature (such as [4]) lay emphasis on the fact that extreme loads are often caused by high turbulence in the wind. The frequencies of the gust must be near the component natural frequencies to play a significant role in the extreme loads computations. Other reports suggest using environmental contours [7] to determine the right wind and wave conditions for identifying the highest peak loads. Also, the highest operating out of plane extreme loads need not be caused purely from environmental inputs as these loads are also a function of the controller behavior and blade aerodynamics. Hence herein, the key mechanisms driving the rotor and mud level out of plane extreme loads are identified, so that their understanding facilitates the creation of the fast computational code.

2. Mechanics of the Simulated Peak Extreme Out of Plane Load

The Upwind turbine is run in two configurations of onshore and offshore with a monopile at a mean water depth of 20m. The simulation is performed in HAWC2 with a normal turbulence wind input. The waves are based on linear theory and generated using the JONSWAP spectrum [2]. To understand the physics of the out of plane loads, the onshore turbine extreme loads are first analyzed. Figure 1 describes the comparison of the highest extreme tower base fore-aft bending moment for a land turbine along with the peak out of plane blade root moment, as a function of the mean wind speed with 20 seeds of 10 minute simulations at each mean wind speed. The extreme loads are seen to possess the highest peaks in the region between rated wind speed (11.4m/s) and about 5m/s above rated wind speed. The tower base out of plane moment also displays increasing extreme loads at cut-out. The extrapolation of the tower base extreme moment can be performed based on the sampled extreme loads from this simulation. The complete aeroelastic simulations take 30-32 hours on a modern computer, for 20 turbulent seeds at each mean wind speed.

The load extrapolation is carried out based on the approximation to the local cumulative distribution function (CDF) as the median rank of the extremes, as in

$$CDF = \frac{i - 0.3}{N + 0.4} \qquad -(1)$$

where i is the sorted index of the extreme load and N is the total number of extreme loads. A parametric fit to the local median rank is made using the Gumbel distribution with a quadratic exponent [8] as the CDF. By computing the probability of exceeding the largest extreme [8] and using a Rayleigh wind distribution with discrete bins (index i refers to each bin), the long term probability of exceedance can be summed up as in Eq. (2): wherein *a, b, c* are the coefficients of the parametric fit to the data with n_i independent samples at a mean velocity of v_i. The extrapolation of the CDF is performed: 1) using one peak extreme per 10 minute simulation. This provides for 20 data points at each mean wind speed. 2) Using 20 seeds per mean wind speed only between 10m/s and 16m/s and tapering the number of turbulent wind seeds to less than 10 at cut-out and below 10m/s. The results of the tower base out of plane moment extrapolation are shown in Fig. 2 which display the extrapolated tower base fore-aft moment is affected only 2% through the reduction in the number of wind seeds for mean wind speeds outside the domain of 10m/s to 16m/s. While the results maybe particular to this specific case, the observation facilitates the understanding that to determine the 50 year

$$P(F_e > F) = \sum_{i=cutin}^{cutout} \{(e^{-\pi\left(\frac{v_i - \Delta v_i/2}{2v_{ave}}\right)^2} - e^{-\pi\left(\frac{v_i + \Delta v_i/2}{2v_{ave}}\right)^2})(1 - (e^{-e^{-(a(v_i)F^2 + b(v_i)F + c(v_i))}})^{n_i})\} \qquad -(2)$$

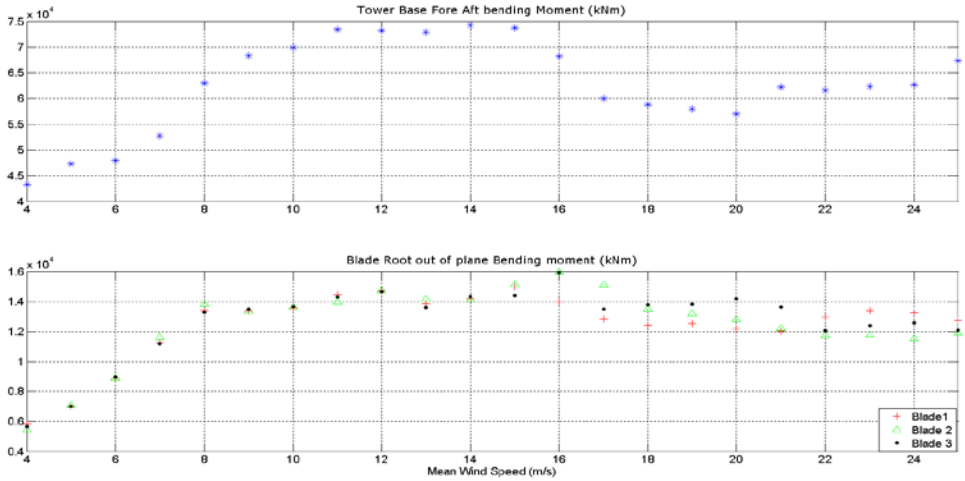

Figure 1 : Variation of the peak blade root out of plane bending moment and the peak tower base fore-aft moment with the mean wind speed

tower base out of plane load for this turbine, the domain of interest on the mean wind speeds is between 10m/s and 16m/s. Further, a consistent reduction in computational efforts can be made by isolating the conditions for the highest tower base fore-aft moment in this mean wind speed domain and utilizing those dependencies in a simplified simulation. To understand the details for the largest tower base fore-aft moment in Fig.1, the specific time histories of that simulation is scrutinized. The dynamics of the angle of attack, tower base bending moments and the blade root moments on all three blades are shown in Fig.3

Investigation of the peak loads in Fig. 1 based on all the simulation parameters reveal three principal mechanisms for the tower base peak out of plane moment:

1. A local high angle of attack on an outboard blade section that is close to the angle of maximum lift as shown in Fig.3.
2. A blade pitch angle close to 0 degrees even at mean wind speeds above rated and
3. At least two blades possessing a significant peak out of plane moment load. Solitary highest blade out of plane moments does not induce the highest tower base out of plane moment, but highest pair blade loadings can induce the largest out of plane tower base moment.

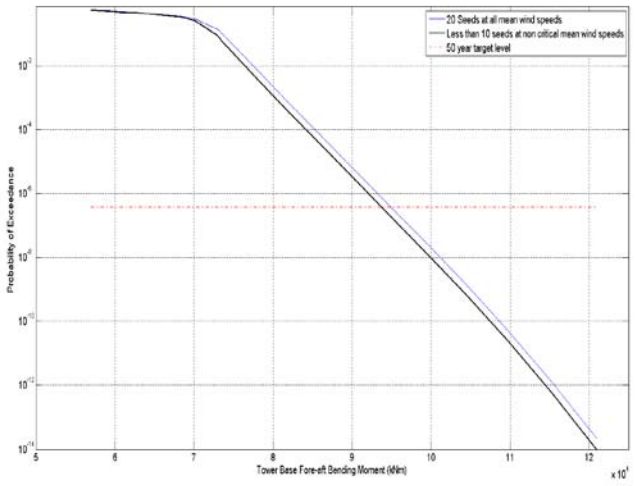

Figure 2: Extrapolation of the Tower base out of plane bending moment

The instant of the highest tower base bending moment is identified and the instantaneous angle of attack variation on one of the blades across the blade span is compared with corresponding angle of attacks at instants with lower tower base moments. This comparison displayed in Fig. 4 reveals that though the blade inboard angle of attack profiles are quite similar, the outboard angle of attack profile at the instant of the peak tower base moment departs from the familiar profile to show marked increase in

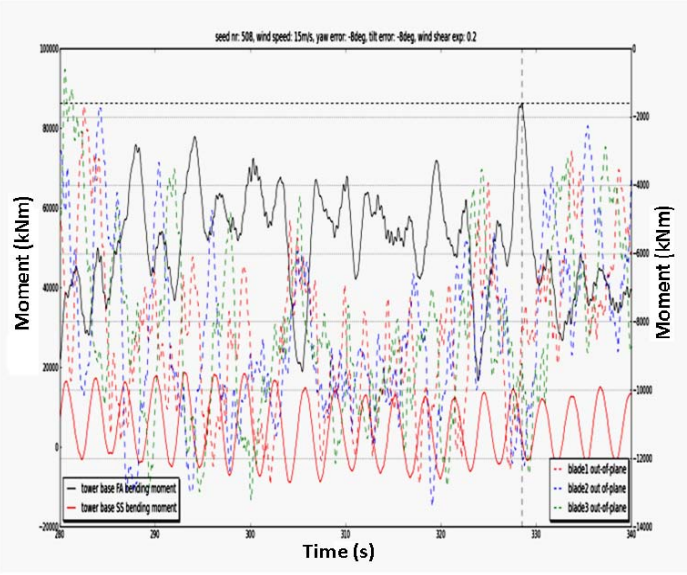

Figure 3 A: Time series analysis of the coincident blade moments at the instant of the peak tower fore-aft bending moment

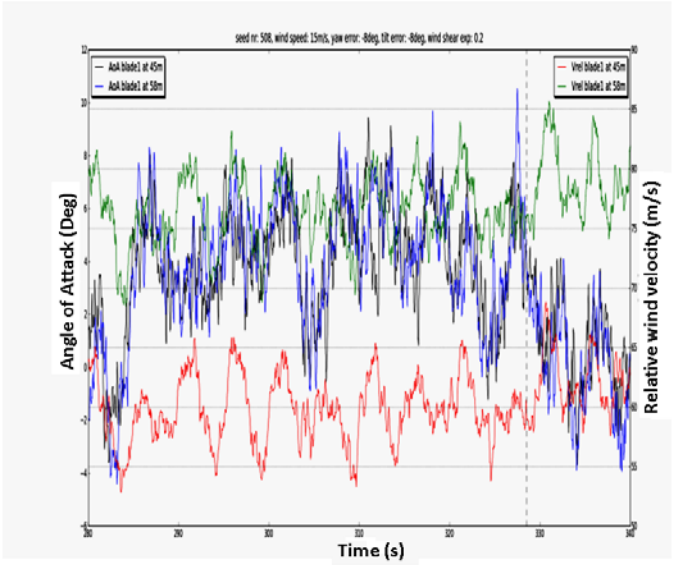

Figure 3 B: Time series analysis angle of attack (AOA) and relative wind speed on the blade (Vrel) at the instant of the peak tower fore-aft bending moment

its magnitude. The reason for the high angle of attack is due to the low blade pitch angles set by the controller in the past few seconds before the occurrence of the peak load. Figure 5 displays the rotor RPM which is below the rated speed for a significant time prior to the instant of the peak tower base moment (at ~329s) and during that interval the blade pitch angle drops below 1 degree which is also the trigger for the generator torque set point. This causes a sudden drop in generator torque even though the rotor torque is above rated. These events cumulatively result in a jump in the angle of attack at the outboard blade stations at this high mean wind speed. Further, due to the turbulence in the wind, a localized increase in wind speed at any position across the blade can now induce a high thrust loading at sections along that blade.

Regardless of the complexity of the control algorithm, if the rotor speed is below rated speed for a sufficient duration, then the instantaneous pitch angle can drop sufficiently low to cause generator torque triggers at mean wind speeds above rated. If a sufficiently advanced controls mechanism is employed in the turbine with loads feedback to the

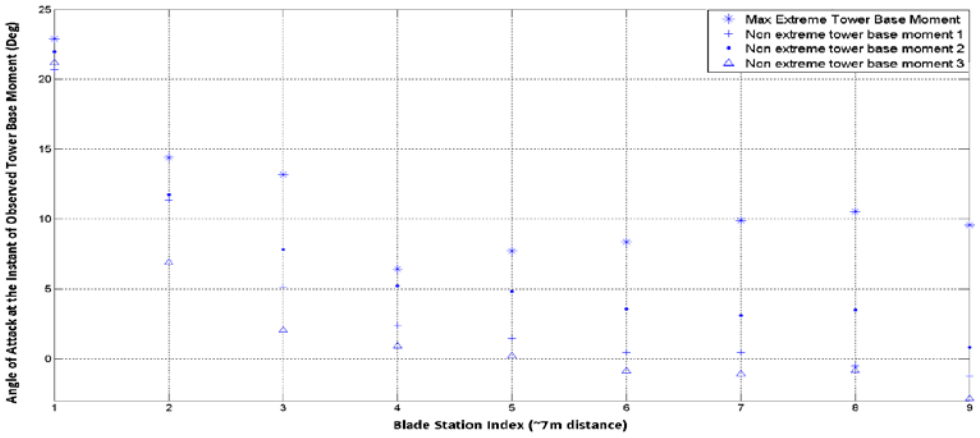

Figure 4: Magnitude of the angle of attack on blade 1 at different blade stations along its span

pitch controller and differential pitching, then based on the increased thrust loading due to the rising angle of attack, the pitch controller may reduce the highest thrust load otherwise attained. However, the impact of such an advanced controller still depends on the time constants of the system and sudden wind turbulence in isolated rotor azimuths can still trigger high thrust loads. Potentially a LIDAR (Laser anemometry) based wind observer may prevent such high angles of attack being developed on the blades, but herein we assume conventional controllers. Based on the above observations that result in the highest tower base out of plane load, a simplified extreme loads code is made that possesses the essential features:

1. The lift, drag curves for the blade airfoils are used. The blade section that possesses the largest chord times lift coefficient is made to attain the maximum lift. Other blade station angles of attack are obtained from blade element momentum theory and conforming to the max angle of attack at one station.
2. The wind power spectral density and coherence function are used jointly with the blade and tower mode shapes at the tower fundamental frequency.
3. Irregular wave loading on the support structure is included.

3. Theoretical Formulation of extreme loads

The load calculations are performed for wind class I B and which is considered to be representative for offshore wind conditions. The turbulent longitudinal wind velocity component spectrum ($S_u(f)$) and its corresponding coherence function is used to derive the extreme load spectral function. The turbulence spectrum used for the analysis is the Kaimal spectrum [1]:

$$S_u(f) = \frac{4\sigma_1^2 L_1/V_{hub}}{(1+6f\,L_1/V_{hub})^{5/3}} \quad -(3)$$

where $\sigma_1=I_{ref}(0.75V_{hub}+5.6)$ is the longitudinal turbulence standard deviation with $I_{ref}=0.14$

L_1: is the longitudinal velocity integral scale $=8.1\Lambda_1$

f: is the frequency in Hertz

$\Lambda_1 = 42m$ is the longitudinal turbulence scale parameter at 90m hub height

The exponential coherence model is used in conjunction with the Kaimal spectrum to account for the spatial correlation of the longitudinal wind speed component:

$$\gamma = \exp\left[-12\sqrt{(f\cdot r/V_{hub})^2 + (0.12\,r/L_1)^2}\right] \quad -(4)$$

where r is the magnitude of the projection of the separation vector between the two points on to a plane normal to the predominant wind direction. The extreme out of plane load can be derived based on the segmentation of the wind velocity into the mean and the variation. Hence the net wind velocity over the blade is

$$V_{nB} = \sqrt{\left(V+\bar{u}\right)^2(1-a)^2 + (1+a')^2(r\omega)^2} \quad -(5)$$

Where V is the mean wind speed at a particular blade station, $\bar{u}$ is the turbulent velocity, ω is the rotor speed, a and a' are the axial and tangential induction factors,

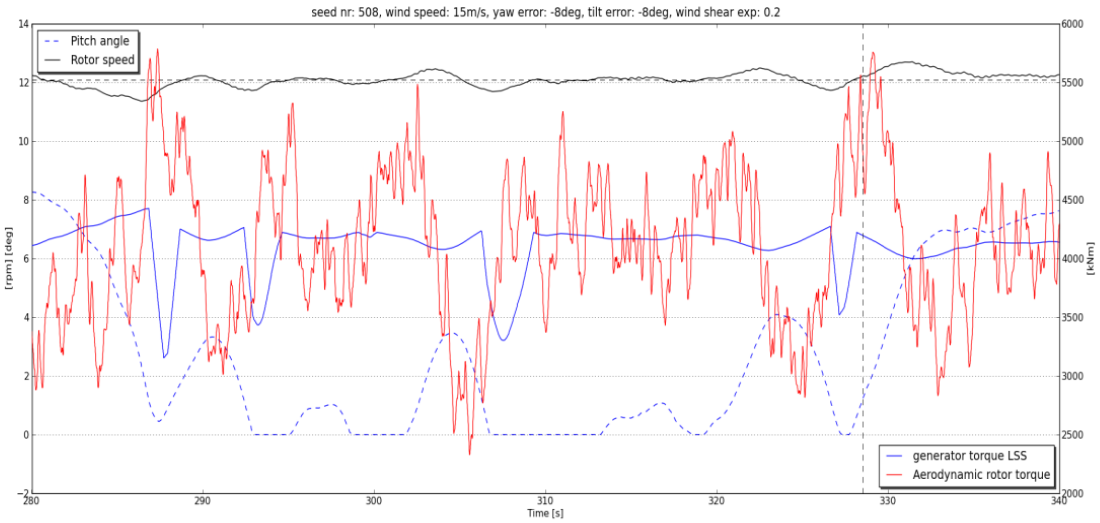

Figure 5 : Dynamics of the pitch angle and generator torque prior to the occurrence of the extreme tower fore-aft moment

which are computed from the equation for mechanical power since most mean wind speeds that are of interest are near or above rated wind speed.

extreme dynamic tower thrust load is given by using Eq. (6) and Eq. (7) along with fundamental random vibration formulation [9] as

$$T(V,z) = T_S(V) + p\rho C_l c \cdot \sqrt{(V_1^{\,2} \cdot W_u(V)_1. + V_2^{\,2} \cdot W_u(V)_2. + V_3^{\,2} \cdot W_u(V)_3.)}\, f_T^{\,2} \cdot \frac{\chi}{(f_T^{\,2} M)} \cdot \sqrt{\frac{\pi f_T}{4\zeta}} . \varphi(z) \mathrm{m(z)} \text{ - (7)}$$

$$\beta(r_1, r_2) = \int_0^R \int_0^R \gamma(r_1, r_2)\psi(r_1)\psi(r_2) dr_1 dr_2$$

$$W_u(V) = S_u(f_T) \cdot \int_0^h \left(\int_0^h [\beta(r_1, r_2)\delta(z_1 - h)\varphi(z_1)] dz_1 \right) \beta(r_1, r_2)\delta(z_2 - h)\phi(z_2) dz_2$$

The mechanical power at the instant of the extreme load is usually seen from simulations to be 2-3% higher than the set point. Similarly the rotor speed amplitude in Fig. 5 is approximately 3% higher than the set point at the instant of the peak thrust load as observed in the aero elastic simulations. This is taken into consideration.

The mean extreme out of plane force at the blade root is determined by using the hub height mean velocity *V* and shear factor, along with the blade lift coefficient at each blade station, wherein a prescribed blade station which has the maximum influence on the thrust attains the highest lift coefficient, i.e.

$$T_S(V) = 3\int_0^R 1/2\rho\left((V(1-a))^2 + \left((1+a')r\omega\right)^2\right) c c_{L\max profil} \cos(\phi_r) dr \quad \text{– (6)}$$

Where T_S is the thrust at the hub, ϕ_r -relative wind direction at each station, $c_{Lmaxprofil}$ – Lift coefficient at each blade station computed when the section that influences the root thrust most, attains the maximum lift, ρ is the air density, and *R* is the rotor radius.

The variation of the extreme out of plane force depends on the admittance function of the turbine structural dynamics. Herein the conventional drag based approach in building codes is departed from [9]. The mud line out of plane moment is mainly driven by the rotor thrust and the wave kinematics and hence though the structural stiffness of the support structure is essential to consider for the derivation of the admittance function of the tower response, the loading is derived from the blade aerodynamics and not the wind loading on the tower. The background load spectrum is further obtained from the wind loading at frequencies below the natural frequency of the structure, but this does not result in a significant dynamic load and hence can be disregarded for the computation of the peak extreme load. Therefore the

Where

ψ – Blade first mode shape

φ – Tower first mode shape

δ - Dirac Delta function

C_l – Lift coefficient at 70% blade span

c – blade chord length at 70% span

χ – blade admittance function = Sears function

M – Total tower mass

m(z) – sectional tower mass

f_T – first tower natural frequency = 0.31 Hz.

ζ - tower structural damping coefficient = 0.01

p = Davenport peak factor

V_1, V_2, V_3 – wind velocities at 70% blade span of each blade.

There are two distinctive aspects of this extreme load formulation that departs from conventional civil engineering practices, 1) The mean out of plane load is based on the location of the blade section that influences the rotor thrust the most and determining the resulting lift coefficient at all other blade stations. The angle of attack profile across the blade is thus developed based on the axial and tangential induction factors and corrected based on the section that attains the maximum lift coefficient. The Øye dynamic stall correction [10] is also used to determine the maximum angle of attack and the maximum lift coefficient.

2) The dynamic variation of the tower base extreme moment is based on the resultant thrust acting at the tower top as a point force and integrated with the tower and blade structural response. The blade elastic and the tower elastic response is together considered using the first mode shape of each component. If there is reason to include higher mode shapes, then such application can be made into Eq. (7).

4. Environmental Conditions

The environmental conditions, specifically the mean wind speed and the significant wave height for the 50 year extreme load are required as inputs for the simplified extreme loads code. This is estimated using the Inverse First Order Reliability Method (IFORM) [7].

As assumed during the process of extreme loads extrapolation in Fig.2, the probability of exceedance for any load is assumed to be represented by its median rank. Thus the environmental contour reduces to a two dimensional polar with its axes containing the mean wind speed and the corresponding significant wave height.

The 50 year probability of failure is 3.8e-7 and assuming a normally distributed failure probability as in IFORM, the β value is 4.95. If the corresponding normal variables for the significant wave height and the mean wind velocity are given by $F_{W|v}$ and F_V, then

$$F_V{}^2 + F_{W|v}{}^2 = \beta^2 \qquad \text{- (8)}$$

and using the Rosenblatt transformation [11]

$$F_V = \Phi^{-1}(P_v) \; and \; F_{W|v} = \Phi^{-1}(P_{w|v}) \qquad \text{-(9)}$$

Where Φ indicates the normal CDF and *P* indicates the Rayleigh distribution for the mean wind speed and the Weibull distribution for the significant wave height conditional upon the mean wind speed.

Using Eq. (8) and the inverse Weibull distributions, the 50 year return contour for the mean wind speed and significant wave height can be generated, assuming that the domain of interest is curtailed to between cut-in wind speed of 4m/s and cut-out wind speed of 25m/s. The wave significant height distribution was based on the observations in Ref. [12] and scaled to the water depth of 20m in the present example.

Figure 6 describes the return contour for the 50 year significant wave height at each mean wind speed curtailed to the domain of wind turbine operation. These environmental conditions can now be utilized in conjunction with Eq. (7) to directly predict the 50 year tower base extreme out of plane load without the need for any extrapolation and without the need for any time domain loads computations.

5. Extreme load Computations

Initial computations are performed without the wave loading to determine the influence of the rotor aerodynamics on the mud line out of plane moment.

Figure 7 displays the maximum extreme mud line out of plane bending moment as a result of executing the simplified code with input wind only and without the impact of waves. This is plotted as a function of the mean wind speed and compared with the extrapolated 50-year load as obtained by using extreme tower base moments from a HAWC2 simulation, again without considering wave loads. Figure 8 displays the 50 year extrapolated extreme mud line out of plane moment

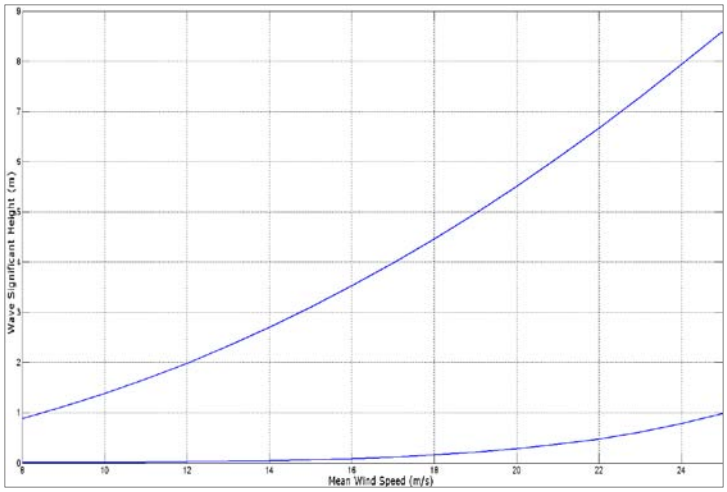

Figure 6: Environmental return contour for the 50 year significant wave height as a function of the mean wind speed

with rotor aerodynamics generated forcing only. The 50 year extrapolated moment at the mud line without waves is 116000 kNm and from Fig. 7, the simplified 50 year out of plane moment at the mud line is 124710 kNm. Thus the simplified code result is 7.5% higher than the extrapolated load value. Such a conservative close estimate of the 50 year tower base out of plane bending moment is beneficial for the designer in the preliminary design phase as the ultimate stress of the component can now be estimated based on this quick computation. The time for obtaining the 50 year extreme load at the mud line using this simplified procedure for wind loading is less than 10 seconds on a modern desktop computer. Wave induced extreme loads on the foundation are now computed using the extreme significant heights as depicted in Fig. 7.

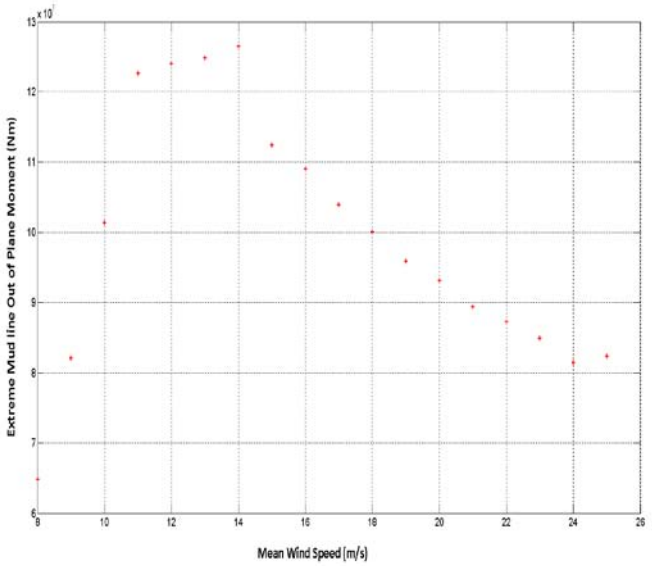

Figure 7: Simulated maximum year extreme mud line out of plane loads using the simplified approach

$$M_{D\max}(\omega, y) = -\left(C_d \frac{1}{2} d\rho\right)^2 \mathrm{S}(\mathrm{H_s}, \omega)\omega^2 \left[\frac{(d+\mathrm{y}) - \mathrm{d}^2\mathrm{k}\,\mathrm{cosech}(\mathrm{d\,k})^2 (k(d-y) + \sinh(2dk))}{4\,\mathrm{k}^2\,(\mathrm{d}+\mathrm{y})}\right]^2 \quad -(12)$$

As is common in industry, the Morison's equation is used to compute the wave loading on the foundation, but herein a linearized version of the Morison's equation for wave loading is used [13] as given by

$$\mathrm{dF}(\mathrm{z}, \mathrm{t}) = \mathrm{C_M}\rho\frac{\pi}{4}\mathrm{d}^2\,\dot{\mathrm{u}}\,\mathrm{dz} + \mathrm{C_{dl}}\mathrm{d}\frac{1}{2}\rho\mathrm{u}\,\mathrm{dz}$$

- (10)

Where C_M is the coefficient of inertia, d is the diameter of the monopile, u is the horizontal wave velocity at the section z and C_{dl} is the linearized coefficient of drag. The monopile displacement velocity and acceleration effects on the wave forcing are not explicitly taken into account as the maximum relative velocity is considered. The linearized drag coefficient for Gaussian waves is estimated for a prescribed std. deviation of velocity (σ_u) [13] as $C_{dl} = 1.596.C_d.\sigma_U$

The C_d and C_M are set to their maximum theoretical values. Based on the value of σ_u, from the JONSWAP spectrum, the linearized drag parameter can be computed. The mud line moment from wave loading can be computed using many methods, but here the mud line extreme moments are estimated using the methods of Wheelers stretching [14] and linear Airy theory. Wheeler's stretching accounts for the effect of the height of the wave above the free surface, but is normally known to under predict the wave velocity and acceleration for high wave heights above the sea level [14]. The linear Airy theory tends to over predict the wave velocity and acceleration for high wave heights above the free surface [14].

The maximum mud line out of plane moment is given by taking the product of Eq. (10) with the vertical distance from the mud line and integrating over the height of the monopile. Assuming Airy linear wave equations with wheeler stretching, the maximum mud line bending moment PSD from inertial wave loading at the baseline is therefore derived readily as

$$M_{\mathrm{Im}ax}(\omega, y) = \left(C_M \rho \frac{\pi}{4} d\right)^2 \left[\frac{(\mathrm{Tanh}(\frac{\mathrm{d\,k}}{2}) - \frac{\mathrm{d}^2\mathrm{k}}{\mathrm{d}+\mathrm{y}})}{\mathrm{k}^2}\right]^2 \omega^4 S(H_s, \omega)$$

- (11)

and the maximum mud line bending moment PSD from the wave drag loading is

where y is the wave elevation above the free water surface and k is the wave length. Since Eq. (11) and (12) are in the frequency domain, their computation is quick given the power spectrum for the wave height. However the wave height above the free surface may need to be iteratively solved or this can be assumed to be equal to the significant height as given in Fig. 6 without great loss of precision.

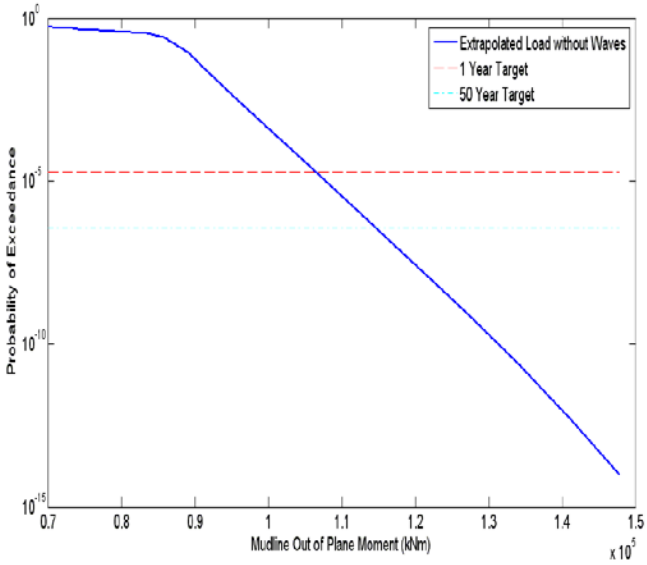

Figure 8 : Extrapolated Mud line out of plane bending moment without wave load contribution

Figure 9 describes the maximum extreme 50 year mud line out of plane moment with wave loading wherein the Wheeler stretching and linear Airy theory without stretching is used to compute the wave loads. As can be seen in Fig 9, up to a mean wind speed of 15m/s, the peak loads from the two wave loading methods match each other's magnitude within 2% of each other, but with higher mean wind speeds, the wheeler's stretched maximum mud line moment is less conservative with wave height.

Since the overall peak mud line moment is near rated wind speed, the peak extreme load value from either wave loading model can be used. A crucial aspect of computing the wave loads using the power spectral density function is the cut-off frequency. Using too high cut-off frequencies will result in unrealistic high loads due to the wave acceleration being proportional to the square of the frequency. As given in Ref. [15],

the cut-off frequencies used herein are given by

$$\omega_C = \sqrt{\frac{2g}{H_S}}$$

The cut-off frequency should be chosen so that at least the first two natural frequencies of the support structure are included. Further the Gaussian time series generated from the power spectrum that is used for any loads series analysis should possess a time step that is consistent with the Nyquist sampling criterion.

6. Comparison with the extrapolated mud line moment

The extreme 50 year loads thus obtained in Fig. 9 is compared with the extreme extrapolated mud line out of plane moments that were computed using HAWC2 simulations with the same significant wave height as given in Fig. 6. Here 7 different turbulent wind seeds were used at each mean wind speed. Similarly the number of irregular wave seeds at each mean wind speed was varied between 3 to 6, which results in a maximum of 42 ten minute simulations at each mean wind speed. The effect of wave loads on the overall extrapolation was found to be beneficial in the parametric fitting, as the spread in extreme loads due to the waves is fairly even as compared to the spread in extreme loads due to only the wind influence.

Figure 10 displays the result of this extrapolation. The 50 year extrapolated mud line out of plane moment is 164000 kNm, whereas in Fig. 9, the peak mud line out of plane moment is 148000 kNm. Therefore the simplified computational tool is able to assess the 50 year mud line load level in the same range as the extrapolated load, but predicts it to be about 10% lower than the extrapolated value. This can be due to the inclusion of the wave loading directly into the extrapolation process. It can be argued that the statistical extrapolation is carried out only on the mud line loads derived from the rotor dynamics and the wave loading can be added to this, since the extreme wave heights in Fig. 6 are being used in the HAWC2 simulations. Based on Figure 9 and Fig.7, the increase in mud line out of plane bending moment with wave and wind loading at the peak level at 13m/s mean wind speed is 19% as compared to the extreme load with wind inputs alone. If the extrapolated 50 year bending moment as influenced by rotor aerodynamics in Fig. 8 is increased by a factor of 19% to account for this peak wave loading, then the 50 year out of plane extreme bending moment at the mud line is 138,000 kNm. If this is taken as the reference extrapolated extreme 50 year moment, then the results from Fig. 9 are only 7%

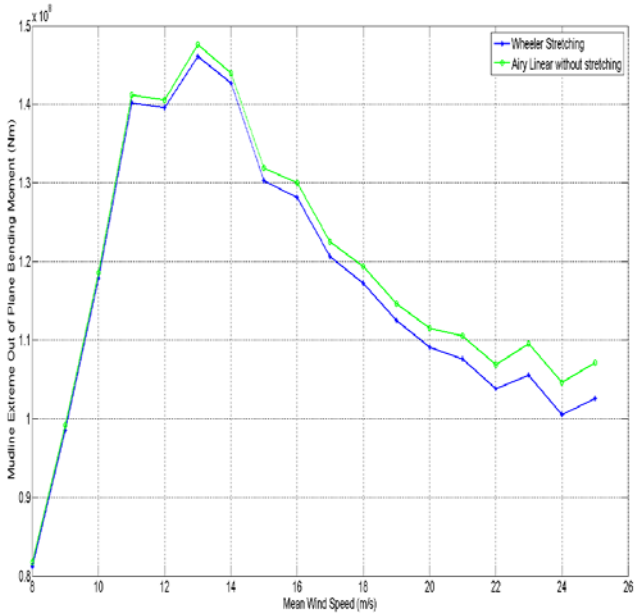

Figure 9 : 50 Year Extreme mud line out of plane bending moment inclusive of wave loading

higher, which is exactly as per the trend in Fig. 7 with the wind dominated extreme moments.

With flexible soil conditions, the impact of the soil stiffness on the support structure frequency determines whether the extreme loads on the support structure will increase. The DNV guidelines [15] describe the soil stiffness based on the friction angle between the soil and the support structure. For the current turbine, a soil friction angle of 30 degrees provides for a reduced frequency of the support structure that is just above the rotor 1P frequency of 0.2 Hz. The corrections to the extreme load results from the simplified code for soil structure interactions can be readily determined based on the corrected mode shapes and frequencies being entered into Eq. (7).

7. Conclusions

A simplified loads code to compute the extreme out of plane loads was developed and verified against the extrapolated mud line out of plane bending moments for a 5MW turbine with a monopile foundation. The extreme tower base bending moment is the result of high angle of attacks occurring on two or more of the blades out board sections simultaneously. These high angles of attacks are caused by control system behaviors that result in low blade pitch angles and subsequent generator torque drops at mean wind speeds above rated.

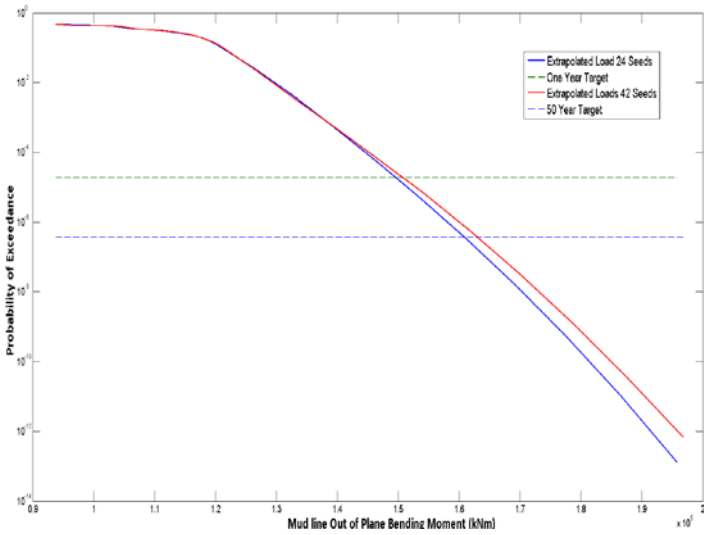

Figure 10: Extrapolated 50 year mud line out of plane moment inclusive of wave loading

The mean extreme load was derived based on the blade angle of attack distribution corrected by the angle of attack at the blade section with the maximum chord times lift coefficient. The dynamic factor to this mean load was determined based on the first mode shape and frequency of the tower in conjunction with the first mode shape of the blade and applied as an impulse force at the tower top. Wave loading based on wheeler stretching and Airy linear were both independently computed on the support structure. The 50 year out of plane mud line moment was verified to be within 10% of the extrapolated out of plane mud line moment when using sampled extremes loads data from HAWC2.

Acknowledgement

The work presented in this paper is part of the Integrated Project "UpWind" supported by the EU sixth Framework Program, grant no. 019945. The financial support is greatly appreciated. Also, the help from David Verelst and Felipe Sanchez of Risø DTU with aeroelastic simulations is gratefully acknowledged.

References

[1]. *International Standard Wind Turbines—Part 1: Design Requirements* IEC 61400–1 Ed. 3. 2005

[2]. *International Standard Wind Turbines—Part 3: Design Requirements for offshore wind turbines* IEC 61400-3 Ed. 1 2009.

[3]. Agarwal, P. and Manuel, L., "Extreme Loads for an Offshore Wind Turbine using Statistical Extrapolation from Limited Field Data", *Wind Energy,* 2008; **11**:673–684

[4]. Moriarty, P., Holley, W.E., Butterfield, S. Effect of turbulence variation on extreme loads prediction for wind turbines", *Journal of Solar Energy Engineering-Transactions of the ASME* , 2002, 124: 387-395

[5]. Jonkman, J. et. al. *Definition of a 5-MW Reference Wind Turbine for Offshore System Development*, Technical report NREL/TP-500-38060, February 2009, Golden, Colorado,

[6]. *Zaaiger, M.B., "Foundation modeling to assess dynamic behavior of offshore wind turbines",* Applied Ocean Research 28 (2006) 45–57

[7]. Saranyasoontorn, K, Manuel, L**, "**Design Loads for Wind Turbines Using the Environmental Contour Method", *Journal of Solar Energy Engineering*, Transactions of the ASME, 2006, Vol. 128, No. 4. 554-561.

[8]. Natarajan A. and Holley, W.E., "Statistical Extreme Load Extrapolation with Quadratic Distortions for Wind Turbines", *Journal of Solar Energy Engineering-Transactions of the ASME*, 2008, 130 (3): 031017

[9]. Zhou, Y. et al., "Equivalent static buffeting loads on structures"**,** Journal of Structural Engineering, August 2000, 989-992.

[10]. Petersen, J.T. et. al. "Prediction of Dynamic Loads and Induced Vibrations in Stall", Risø National Laboratory report No. Risø-R-1045(EN), 1998.

[11]. Rosenblatt, M., "Remarks on a Multivariate Transformation*," Annals of Mathematical Statistics*, 1952, Vol. 23, No. 3, 470-472.

[12]. Johannessen, K., et. al., "Joint Distribution of the Wind and Waves in the Northern North Sea*", 11th International Offshore and Polar Engineering conference*, 2001.

[13]. Veer, R.V., "Application of Linearized Morison Load in Pipe Lay Stinger Design", *ASME 27th International Conference on Offshore Mechanics and Arctic Engineering, 2008*

[14]. Randall, R.E., Zhang,J. and Longridge, J.K., "Laser Doppler Anemometer Measurements of Irregular Water Wave Kinematics*", Ocean Engineering*, 1993, Vol. 20. No.6, 541-553.

[15]. *Design of offshore wind turbine structures,* DNV-OS-J101, Oct. 2007, 125-128.